Solution of a Multinephron, Multisolute Model of the Mammalian Kidney by Newton and Continuation Methods

RAYMOND MEJIA AND JOHN L. STEPHENSON
Section on Theoretical Biophysics, National Heart, Lung, and Blood Institute, and Mathematical Research Branch, National Institute of Arthritis, Diabetes, and Digestive and Kidney Diseases, National Institutes of Health, Bethesda, Maryland 20205

ABSTRACT

A method of numerically solving the differential equations specifying solute and water flow in a multinephron, multisolute model of the mammalian kidney by a combination of Newton and continuation techniques is described. This method is used to generate a connected component of the steady state solution manifold of the model. A three dimensional section of this manifold is shown to be convoluted, with upper and lower sheets of stable solutions connected by an unstable middle sheet. Two dimensional sections of this surface are followed from a trivial constant profile of concentrations in the nonconcentrating kidney to the profiles of the maximally concentrating kidney. Study of these sections shows that for a given choice of model parameters there may exist no solution, there may be a unique solution, or there may be multiple solutions. A study of the time dependent solutions shows that the dynamic transition from the lower to the upper state and return may be via a hysteresis loop.

---

1. INTRODUCTION

In previous papers and conference reports we have described various aspects of a multinephron model of the kidney [15–17,29,30], and we have shown that this model as well as simpler prototype models may have multiple steady state solutions [18,31]. We have also described our numerical methods [13,14,16,18,27,28,33,34] and have compared them with other techniques [10,13,14,19]. In recent papers other authors have described various alternative schemes of solving the differential equations of kidney models [2,5,7,10,11,20].

In this paper we show how our previously developed Newton methods may be combined with a continuation method to arrive at solutions of the model equations. The development of this method serves two general pur-

poses: First, it permits us to converge to a solution with an initial estimate that is far from the final solution. Secondly, it permits the solution of the model to be followed as a function of any selected model parameter. To illustrate the technique, we construct a two dimensional section of the solution manifold in which the solute concentrations are exhibited as a function of the ratio of nephrons with short loops of Henle to those with long loops of Henle and of the hydraulic permeability of the collecting ducts of the short nephrons. In doing so we show how to develop a steady state solution for a given choice of parameters starting with the boundary values as the initial data.

2. STATEMENT OF THE MODEL

Consider a kidney consisting of many nephrons and separated into an inner (medullary) and an outer (cortical) region (Figure 1). Each nephron is modeled as a separate nephrovascular unit. The model includes two groups
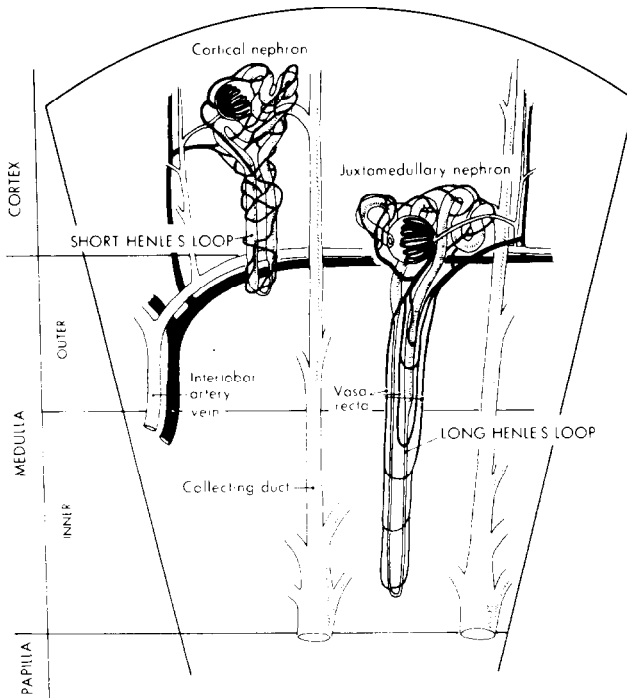

FIG. 1.   Schematic of a sagittal section of the mammalian kidney showing two nephron populations (adapted [22]).

of nephrons: those with short loops of Henle that extend to the junction of the inner and outer medulla, and those with long loops that extend to the papilla. Except for exchange of water and solutes through a common interstitium, each type of nephron functions as a separate nephrovascular unit (Figure 2). After leaving the glomerulus, each efferent arteriole splits into a postglomerular capillary, which exchanges with the cortical interstitium, and a vas rectum, which exchanges with the medullary and cortical interstitium. The vas rectum of each nephron is assumed to penetrate the medulla to the same depth as its loop of Henle. Input data for the model are the arterial, venous, and bladder hydrostatic pressures, and the concentrations of various solutes, which in the calculations to be described in this paper are salt, urea, and protein. The various flow tubes representing renal tubules and capillaries exchange through cortical and medullary interstitia. The cortical interstitium is assumed to be a well-stirred bath; the medullary interstitium is assumed to behave as a flow tube closed at the papillary end and open at the cortical medullary junction. It is assumed to be well stirred in cross section, but in the axial direction there is transport by both convective flow and diffusion.

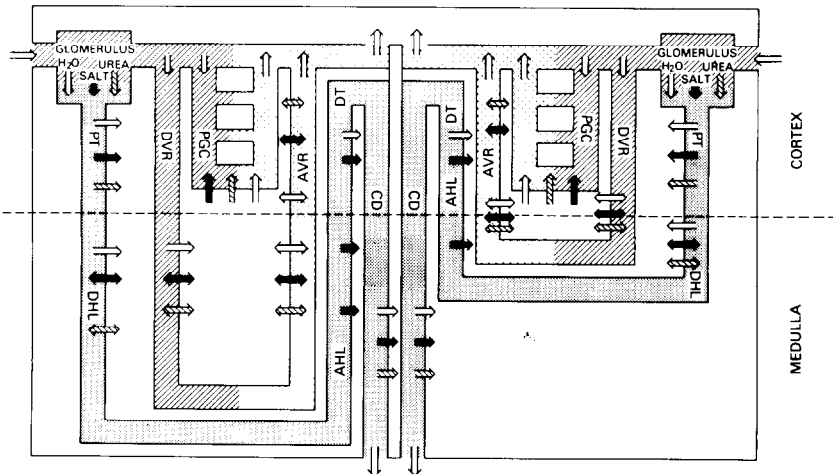## SOLUTE AND WATER MOVEMENT IN THE KIDNEY

FIG. 2.   Schematic of two nephrovascular units. Open arrows indicate transmembrane water flux; solid arrows indicate transmembrane salt flux; hatched arrows indicate transmembrane urea flux. In addition to salt and urea concentration, hydrostatic pressure, concentration of unfiltered proteins, and concentration of a third (possibly impermeant) filtrate are computed.

The differential equations that describe solute and water movement in the ith tubular segment [23–25,27,28] are

$$\frac{\partial}{\partial x}\left(C_{ik}F_{iv} - D_{ik}\frac{\partial C_{ik}}{\partial x}\right) + J_{ik} + \frac{\partial}{\partial t}(A_i C_{ik}) = A_i s_{ik}$$

(species conservation), (2.1)

$$\frac{\partial F_{iv}}{\partial x} + J_{iv} + \frac{\partial A_i}{\partial t} = 0$$

(volume conservation), (2.2)

$$\frac{\partial P_i}{\partial x} + R_i F_{iv} = 0$$

(equation of motion) (2.3)

for $0 \leqslant i \leqslant I$, $1 \leqslant k \leqslant K$, where x is the axial distance along the tube; $0 \leqslant x \leqslant l_i \leqslant 1$; l_i is the length of the ith tube; $0 \leqslant C_{ik}$ is the concentration of the kth solute in the ith tube; F_{iv} is the axial volume flow; D_{ik} is the diffusion coefficient of the kth solute in the ith tube; J_{ik} is the transmembrane solute flux; t is time; A_i is the cross sectional area of the tube; s_{ik} is the average net rate at which the kth solute is being produced or destroyed by physical or chemical reaction; J_{iv} is the transmembrane volume flux (which is assumed to be approximately equal to the water flux); P_i is the hydrostatic pressure; and R_i is the resistance to flow.

The transmural flux laws are

$$J_{iv} = h_{iv}\left[\sum_k RT(C_{qk} - C_{ik})\sigma_{ik} + P_i - P_q\right]$$ (2.4)

and

$$J_{ik} = h_{ik}(C_{ik} - C_{qk}) + \frac{(1 - \sigma_{ik})J_{iv}(C_{ik} + C_{qk})}{2} + \frac{a_{ik}}{1 + b_{ik}/C_{ik}},$$ (2.5)

for $1 \leqslant i \leqslant I$, $1 \leqslant k \leqslant K$, where h_{iv} is the hydraulic permeability coefficient of the ith tube for the kth solute; h_{ik} is the solute permeability of the ith tube for the kth solute; R is the gas constant; T is the absolute temperature; subscript q indicates an interstitial variable (for cortex $q = c$ and for medulla $q = 0$); σ_{ik} is the Staverman reflection coefficient of the wall of the ith tube for the kth solute. The last term in Equation (2.5) defines the metabolically driven transport, which is assumed to obey Michaelis-Menten kinetics; a_{ik} is the maximum rate of transport, and b_{ik} is the Michaelis constant.

Tubes i, $1 \leqslant i \leqslant I$, refer to the nephrons and vasculature of the model. In general, we assume that $s_{ik} \equiv 0$ for all i and k; that $A_i = $ constant for all i;

and that $D_{ik} = 0$ for $1 \leqslant i \leqslant I$ and all k. The equations of the tubes are integrated along each tube in the direction of flow: in the renal tubules from Bowman's capsule (proximal) to bladder (distal), in the capillaries from renal artery (proximal) to renal vein (distal). Boundary conditions are specified at the proximal end of each tube. Thus the volume and solute inflow at the proximal end of each segment must match the outflow of the preceding segment. In the medulla $x = 0$ at the corticomedullary junction and $x = 1$ at the papilla. The sign convention adopted is that flow toward the papilla is positive, and flow away from the papilla is negative. Thus, if the proximal end of tube j is connected to the distal end of tube i, where $F_{iv} > 0$ and $F_{jv} > 0$ (that is, volume flow from tube i into tube j is in the direction of increasing x), e.g. proximal tubule into descending Henle's limb, then

$$C_{jk}(x_0) = C_{ik}(l_i), \qquad 1 \leqslant k \leqslant K, \tag{2.6}$$

$$F_{jv}(x_0) = F_{iv}(l_i), \tag{2.7}$$

$$P_j(x_0) = P_i(l_i). \tag{2.8}$$

If the proximal end of tube j is connected to the distal end of tube i so that $l_j = l_i$ is a turning point, e.g. descending limb of Henle to ascending limb of Henle, then

$$C_{jk}(l_j) = C_{ik}(l_i), \qquad 1 \leqslant k \leqslant K, \tag{2.9}$$

$$F_{jv}(l_j) = - F_{iv}(l_i), \tag{2.10}$$

$$P_j(l_j) = P_i(l_i). \tag{2.11}$$

As observed above, the interstitial space separating the various tubules in the medulla is treated as a tube with a closed papillary end. Hence, Equations (2.1)–(2.3) apply. The boundary conditions for the interstitium are taken to be

$$P_0(0) = P_c, \tag{2.12}$$

$$F_{0v}(1) = F_{0k}(1) = 0, \tag{2.13}$$

$$C_{0k}(1) = \frac{J_{0k}(1)}{J_{0v}(1)}, \tag{2.14}$$

for $1 \leqslant k \leqslant K$ and $F_{0k} = F_{0v}C_{0k} - D_{0k} \partial C_{0k}/\partial x$ (where subscript 0 indicates a medullary variable and c a cortical one). In addition, water and mass conservation require that

$$J_{0v}(x) = - \sum_i J_{iv}(x) \tag{2.15}$$

and

$$J_{0k}(x) = - \sum_i J_{ik}(x) \qquad (2.16)$$

for $0 \leqslant x \leqslant 1, 1 \leqslant k \leqslant K$, where the sums are taken over the tubes that extend to medullary level x.

The cortical interstitium is considered to be a well-stirred bath with hydrostatic pressure P_c and fixed volume V_c. Fluid balance in the cortex requires that

$$J_{cv} \equiv - \sum_i \int_0^{l_i} J_{iv}(x)\, dx = - F_{0v}(0), \qquad (2.17)$$

and solute balance requires that

$$V_c \frac{\partial C_{ck}}{\partial t} + F_{0k}(0) + J_{ck} = 0, \qquad 1 \leqslant k \leqslant K \qquad (2.18)$$

with $J_{ck} \equiv - \sum_i \int_0^{l_i} J_{ik}(x)\, dx$. Again, the sums are taken over tubes that reside in the cortical region.

In modeling proximal tubule transport, it is assumed that transmural transport is isotonic, i.e.,

$$J_M = J_v C_M, \qquad (2.19)$$

where C_M is the total osmolality of proximal tubular fluid. In our calculations on the model, we have assumed various empirical laws for J_v in the proximal tubule; in particular

$$J_v = A + BF_v, \qquad (2.20)$$

where A and B are arbitrary constants.

Equations (2.19) and (2.20) are not intended as a substitute for a detailed model of proximal tubule transport. In the development of the model they serve a "dummy" role for which a more sophisticated model of tubule solute and water transport can eventually be substituted.

It will be noted that implicit in the above equations is the assumption that at a given position along a capillary or tubule, transmural solute and volume exchange are radially symmetric.

For Bowman's space we have the equations

$$\frac{\partial (V_B C_{Bk})}{\partial t} = \int_0^1 J_{Gk}(x)\, dx - J_{Bk} - C_{Bk} F_{PT,v}(0), \qquad (2.21)$$

and

$$\frac{\partial V_B}{\partial t} = \int_0^1 J_{Gv}(x)\, dx - J_{Bv} - F_{PT,v}(0), \tag{2.22}$$

where V_B is the volume of Bowman's space, C_{Bk} is the concentration of the kth solute in Bowman's space, J_{Gk} is transmural flux from glomerular capillary to Bowman's space, J_{Bk} is transmural flux from Bowman's space to cortical interstitium, and $F_{PT,v}(0)$ is volume flow from Bowman's space into the first segment of the proximal tubule.

In the calculations described in this paper we have made certain simplifying assumptions: we have assumed the volume of the kidney and the cross sectional area of the various tubes to be constant; we have also assumed that there are no chemical sources and that diffusion is negligible in tubules. Under these assumptions some of the above equations simplify considerably; e.g. Eq. (2.1) becomes

$$\frac{\partial(F_{iv}C_{ik})}{\partial x} + J_{ik} + A_i \frac{\partial C_{ik}}{\partial t} = 0. \tag{2.23}$$

3. NUMERICAL SOLUTION BY NEWTON'S METHOD

For solution, the system of differential equations (2.1)–(2.3) is replaced with a system of finite difference equations [13,16] as shown below. We select a mesh spacing Δx and divide the interval $[0, l_i]$ into $J_i = l_i/\Delta x$ subintervals with $1 \geqslant l_i$, the length of the ith tubule. A time increment Δt is chosen, so that $t_n = n\,\Delta t$ for $n = 0,1,\ldots$. Let $F_{iv}^n(j)$ denote the approximate value of $F_{iv}(j\Delta x, t_n)$ for $j = 0,1,\ldots,J$, and write the other unknowns similarly. Then the difference equations used, which are centered in space and backward in time, are as follow:

$$\frac{F_{ik}^n(j) - F_{ik}^n(j-1)}{\Delta x} = -\frac{1}{2}\left\{ [J_{ik}^n(j) + J_{ik}^n(j-1)] \right.$$

$$\left. + \frac{C_{ik}^n(j) - C_{ik}^{n-1}(j) + C_{ik}^n(j-1) - C_{ik}^{n-1}(j-1)}{\Delta t} \right\},$$

$$\tag{3.1}$$

$$\frac{F_{iv}^n(j) - F_{iv}^n(j-1)}{\Delta x} = -\tfrac{1}{2}[J_{iv}^n(j) + J_{iv}^n(j-1)], \tag{3.2}$$

$$\frac{P_i^n(j) - P_i^n(j-1)}{\Delta x} = -\tfrac{1}{2}R_i[F_{iv}^n(j) + F_{iv}^n(j-1)] \tag{3.3}$$

for $0 \leqslant i \leqslant I$, $1 \leqslant j \leqslant J$, $1 \leqslant k \leqslant K$. This scheme is $O(\Delta x^2)$ accurate and has been shown to be stable and accurate in approximating solutions of these equations [14].

To solve the above system of finite difference equations we denote the vector of concentrations, pressures, and volume flows for the nth time step by γ^n, and the system of equations by ϕ. We then seek a solution γ^n of the system of equations

$$\phi\left(\gamma^n, \gamma^{n-1}\right) = 0, \tag{3.4}$$

where γ^{n-1} is known either as a set of initial values or from a previous time step. In the steady state $\gamma^n = \gamma^{n-1}$, so we seek a solution of the system of equations

$$\phi\left(\gamma^\infty, \gamma^\infty\right) = 0, \tag{3.5}$$

where by γ^∞ we indicate the steady state vector of unknowns.

The inclusion of several nephrons does not alter the general method of solving Equation (3.4) or (3.5). Here we have found a variant of Newton's method [21] most useful. (See the Appendix.) Thus, to solve the transient equation (3.4) we can make an initial estimate γ_0^n of γ^n. If the norm of the vector $\phi(\gamma_0^n, \gamma^{n-1})$ is less than some preset tolerance, we are through. If not, we improve our estimate of γ^n by repeatedly solving the system of linear equations

$$\phi\left(\gamma^n, \gamma^{n-1}\right) - \Gamma\Delta\gamma^n = 0, \tag{3.6}$$

where Γ is an approximation to the Jacobian matrix $\{\partial\phi_i/\partial\gamma_j\}$ evaluated at γ^n. Computational efficiency demands that any sparseness in Γ be exploited. There are various ways of doing this [13,18,33,34]. The method we have found most useful is to partition the unknowns into two groups [13,17,18]. The first group consists of the unknowns describing the variables along each tube, denoted by γ_i for the ith tube. The second group consists of the global variables, denoted by γ_G, which include the interstitial variables and the three unknowns per nephron that are associated with the exit boundary conditions, which are the venous and the bladder pressure; namely, arterial flow, filtration fraction, and the partitioning of volume flow between the vas rectum and the post glomerular capillaries. Noting that the difference equations for the ith tube involve only the unknowns in the ith tube and the global variables, we may write the equations for the problem in the form

$$\phi_i\left(\gamma_i^n, \gamma_i^{n-1}, \gamma_G^n\right) = 0, \qquad i = 1, 2, \ldots, I, \tag{3.7}$$

$$\phi_G\left(\gamma_1^n, \gamma_2^n, \ldots, \gamma_I^n, \gamma_G^n, \gamma_G^{n-1}\right) = 0. \tag{3.8}$$

Given an estimate of γ_G^n, Equation (3.7) is solved to obtain γ_i^n for each i. Knowing γ_i^n for all i, we then solve (3.8) to obtain a new estimate for γ_G^n. This

process is repeated until γ_G^n is obtained to the desired accuracy. Time is then stepped forward and the entire procedure is repeated. Conditions for convergence are given in [34].

4. CONTINUATION METHODS

Although in general the method described above has worked well for a variety of models, the problem has frequently arisen that the domain of convergence is small, i.e., the starting vector has to be very close to a solution for Newton's method to converge. If not, the successive iterates may either not converge or converge to an inappropriate solution, e.g. a solution with negative concentrations or reversed volume flow in one or more of the flow tubes of the model. To circumvent these problems we have used one of two approaches. The first is to solve the corresponding transient problem [16]. Although this may converge to a solution, unless one is interested in the transient behavior of the system for the particular problem under consideration, it requires a large amount of useless computation. An alternative approach is to use some continuation method. The general idea in these methods as described by Ortega and Rheinboldt [21] is to follow the solution path of a sequence of problems that depend on some continuation parameter α, which may or may not arise naturally from the problem at hand. When $\alpha = \alpha_0$, it defines a problem with a known solution; when $\alpha = \alpha_N$, it defines the problem for which a solution is sought. This idea has been extended recently in a number of papers to include turning points and bifurcations, e.g. Chow, Mallet-Paret, and Yorke [3] and Keller [8]. We have used for this purpose an algorithm of Kubiček [9] as modified by Bunow and Kernevez [1].

To proceed more formally, let $\gamma \in R^m$ denote the vector of m unknown concentrations, pressures, and volume flows arising from a discretization of the differential equations and conservation laws described above, and let $\phi(\gamma) = 0$ be the collection of m discrete equations. Thus, ϕ is a map from R^m to R^m. For continuation we construct a map $\rho(\gamma, \alpha): R^{m+1} \to R^m$, where α is a continuation parameter such that $\rho(\gamma, \alpha_N) = \phi(\gamma)$, and such that the system $\rho(\gamma, \alpha_0) = 0$ has a known solution γ_0. The system $\rho(\gamma, \alpha) = 0$ consists of m equations in $m+1$ unknowns; consequently the locus of solutions, $\rho^{-1}(0)$, is in general a curve. Starting on this curve at $\alpha = \alpha_0$ and $\gamma = \gamma_0$, and numerically calculating points along the curve, one seeks to reach a point on the curve with $\alpha = \alpha_N$, and a corresponding γ_N that is a solution of the system $\phi(\gamma) = 0$.

To define the function ρ there are many possibilities. The functions we have used have been constructed in one of two ways. First, if $\gamma_0 \in R^m$ is a prescribed point, set

$$\rho(\gamma, \alpha) = \alpha\phi(\gamma) - (1 - \alpha)(\gamma - \gamma_0). \tag{4.1}$$

This simple construction, when successful, enables one to start from any point γ_0 in state space with $\alpha = 0$ and to continue along the curve to a point where $\alpha = 1$ and $\rho(\gamma, 1) = \phi(\gamma)$. Equation (4.1) has been used by us to obtain some of our results [18]. For the second choice of ρ, recall that the discrete equations, represented by the function ϕ, contain many parameters, such as permeabilities, pump rates, reflection coefficients, etc. Let us select one of these parameters, denote it by α, and regard $\phi = \phi(\gamma; \alpha)$ as a function of α as well as γ. Then we define

$$\rho(\gamma, \alpha) \equiv \phi(\gamma; \alpha) \qquad (4.2)$$

This choice of ρ enables us to continue a solution that has previously been found, e.g. by the use of Equation 4.1. All the points on the curve are of potential interest, provided the solution (γ, α) stays within reasonable limits, e.g. concentrations remain positive. Some of our results have been obtained through the use of (4.2).

Naively, one could trek along the curve by incrementing α from α_i to $\alpha_{i+1} = \alpha_i + \Delta\alpha$ and then using a Newton scheme to converge to a solution, but it is usually more efficient to utilize the assumed continuity and differentiability of ρ in γ and α to derive the differential equations

$$\frac{d\gamma}{d\alpha} + \Gamma^{-1}\frac{\partial\rho}{\partial\alpha} = 0, \qquad \gamma(0) = \gamma_0, \qquad (4.3)$$

where

$$\Gamma \equiv \left\{\frac{\partial\rho_i}{\partial\gamma_j}\right\} \text{ and } \frac{\partial\rho}{\partial\alpha} \equiv \left(\frac{\partial\rho_1}{\partial\alpha}, \ldots, \frac{\partial\rho_m}{\partial\alpha}\right)^T, \qquad 1 \leq i, j \leq m. \qquad (4.4)$$

If $\Gamma(\gamma(\alpha), \alpha)$ is nonsingular in the interval (α_0, α), then the vector of state variables $\gamma(\alpha)$ obtained by the integration of (4.3) is a solution of $\rho(\gamma(\alpha), \alpha) = 0$ in that interval. If, however, Γ is singular, which occurs at a turning or branching point, this integration scheme fails. To overcome this problem we use Kubiček's algorithm [9] as extended by Bunow and Kernevez [1] to exchange the role of α and a dependent variable γ_i and so obtain a nonsingular matrix.

The central idea of the Kubiček scheme is a parametrization with respect to the arc length s of the solution locus. If, following Kubiček, we differentiate the system of equations ρ with respect to s, we obtain the system of equations

$$\frac{d\rho_i}{ds} = \sum_{j=1}^{m}\frac{\partial\rho_i}{\partial\gamma_j}\frac{d\gamma_j}{ds} + \frac{\partial\rho_i}{\partial\alpha}\frac{d\alpha}{ds} = 0, \qquad i = 1, 2, \ldots, m \qquad (4.5)$$

The additional equation

$$\left(\frac{d\gamma_1}{ds}\right)^2 + \cdots + \left(\frac{d\gamma_m}{ds}\right)^2 + \left(\frac{d\alpha}{ds}\right)^2 = 1, \tag{4.6}$$

determines the parameter s as arc length along the solution curve in R^{m+1}.

In theory, in the system (4.5) of m linear equations, any one of the $m+1$ unknowns $\gamma_1, \ldots, \gamma_m, \alpha$ can be selected as the independent variable and the system solved with respect to it if the corresponding matrix is nonsingular. In the algorithm, the variable is chosen so as to enhance numerical stability. Let γ_k be the new independent variables, and let the matrix

$$\Gamma_k = \begin{pmatrix} \dfrac{\partial\rho_1}{\partial\gamma_1} & \cdots & \dfrac{\partial\rho_1}{\partial\gamma_{k-1}} & \dfrac{\partial\rho_1}{\partial\gamma_{k+1}} & \cdots & \dfrac{\partial\rho_1}{\partial\gamma_{m+1}} \\ \vdots & & \vdots & \vdots & & \vdots \\ \dfrac{\partial\rho_m}{\partial\gamma_1} & \cdots & \dfrac{\partial\rho_m}{\partial\gamma_{k-1}} & \dfrac{\partial\rho_m}{\gamma_{k+1}} & \cdots & \dfrac{\partial\rho_m}{\partial\gamma_{m+1}} \end{pmatrix} \tag{4.7}$$

be nonsingular, where we have designated $\gamma_{m+1} \equiv \alpha$ for consistency. We can then solve the system (4.5) to give the equations

$$\frac{d\gamma_i}{ds} = \beta_i \frac{d\gamma_k}{ds}, \qquad i = 1, 2, \ldots, k-1, k+1, \ldots, m+1. \tag{4.8}$$

Substitution of (4.8) into (4.6) gives the result

$$\frac{d\gamma_k}{ds} = \pm \left(1 + \sum_{\substack{i=1 \\ i \neq k}}^{m+1} \beta_i^2\right)^{-1/2}. \tag{4.9}$$

In (4.9) the sign of $d\gamma_k/ds$ is determined so as to preserve the monotonicity of γ_k along the curve. Substitution of $d\gamma_k/ds$ into the equations (4.8) then determines the derivatives $d\gamma_i/ds$. The integration of the system of differential equations (4.8) and (4.9) is carried out with an explicit Adams-Bashforth multistep method with an automatic change in the order of approximation up to order 4. The truncation error that develops as the integration proceeds is corrected by applying one or more Newton iterations. Further details plus FORTRAN code are given by Kubíček [9].

At singular points, we use the criterion due to Crandall and Rabinowitz [4], to distinguish turning points from simple bifurcations, where the locus of solutions $\rho^{-1}(0)$ consists of two curves that cross at a point. It should be noted that so far in the kidney models no bifurcations have been found.

As shown in previous publications [6,18,32] and in the next section, multiple steady states have been found for a number of models of interest. In the case of two or more steady states, solution of the corresponding time dependent problem has often led to the identification of a solution as being unstable. In the case of multiple stable steady states, a substantial difference in thermodynamic energy requirements [26,27] would differentiate the states, but so far this has not been found. Another means of characterizing solutions is to study the shape of the solution surface and the path from one state to another on this surface.

5. CALCULATIONS

To illustrate our numerical procedures, we give in Figures 3 through 6 the results of some calculations on the model described in Section 2. Tables 1 through 3 show the (normalized) parameter set for the model. Note that there is no active salt transport in the inner medulla; all active transport is restricted to the thick ascending limb of Henle and to the distal tubule. Thus all salt transport out of the thin ascending limb of Henle is by passive diffusion. To arrive at a first point of the section of the solution surface shown in Figure 3 from the boundary values we used the following procedure.
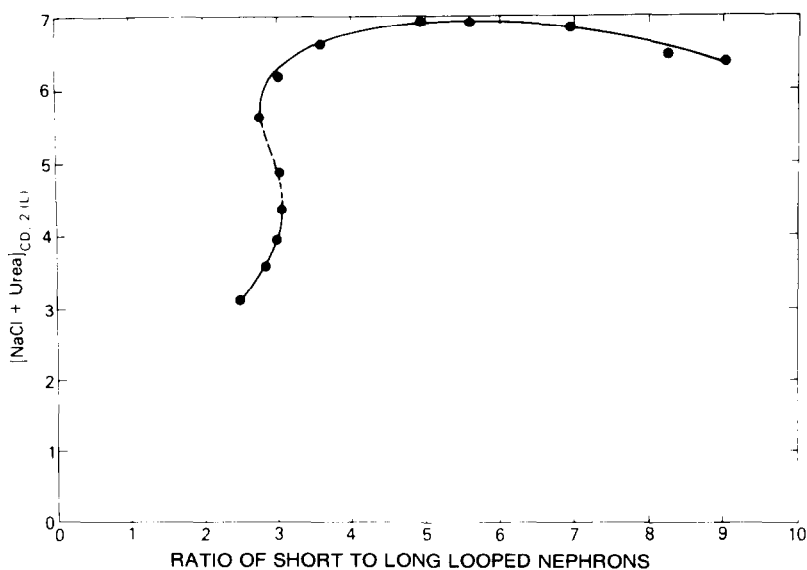

FIG. 3.   Total urine concentration as a function of the ratio of short to long looped nephrons. See text for discussion.
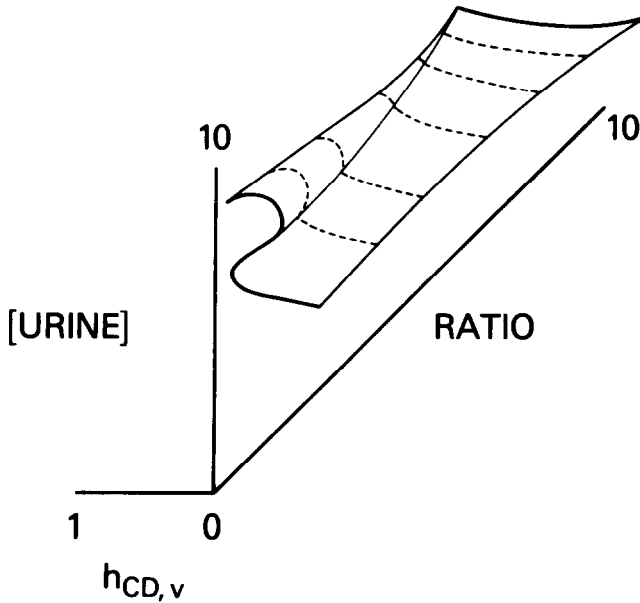
FIG. 4. Three dimensional representation of the solution surface of the multinephron model showing final urine concentration [URINE] as a function of the hydraulic permeability of the collecting duct of the cortical nephron ($h_{CD,v}$) and of the RATIO of short to long looped nephrons.

(a) Set the maximum rate of transport in each tube to zero and the urea permeabilities of the cortical and medullary vasa recta to 10 and 1, respectively. Let γ_0 be the boundary values. Then solve the equations (4.1) for $0 \leqslant \alpha \leqslant 1$. One step is adequate, so we solve the system of equations (3.7) and (3.8) once. This solution has nearly constant concentration profiles, which serve as a good initial approximation in the transition to a concentrating (diluting) kidney. The arterial volume flow, the filtration fraction, the split between the cortical and medullary vasculature, and the hydrostatic pressure profiles have now been essentially established; subsequent changes will be relatively small.

(b) Using the solutions of step (a) as the initial data, solve the equations (4.2) with the maximum rate of salt transport from the ascending loop of Henle for the juxtamedullary nephrons as the continuation parameter. This will yield a solution with the desired final value of $a = 0.6$ in the thick limb.

(c) Using these data, solve the equations (4.2) now with the maximum rate of salt transport from the ascending Henle's limb of the cortical
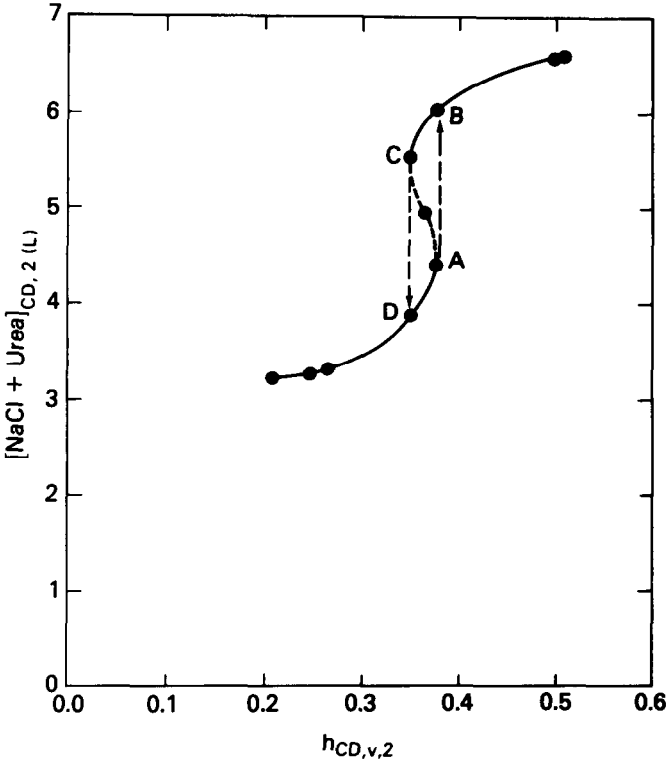
FIG. 5. Total concentration of final urine as a function of the hydraulic permeability of the collecting duct of the cortical nephrons, with the ratio of short to long nephrons fixed at 3.5 to 1. Note the hysteresis type path *ABCDA* indicated by the arrows.

nephrons as the parameter. The path on the solution surface can be continued as long as $c_{ik} \geqslant 0$ for all i and k.

(d) Fix the maximum rate of salt transport from the distal tubule of the long nephrons at the final value, $a = 0.3$. Using the results of step (c) as the initial data, solve the equations (4.1) for $0 \leqslant \alpha \leqslant 1$. One step in α is sufficient.

(e) Fix the maximum rate of salt transport from the distal tubule of the short nephrons at the final value, $a = 0.45$. With the results of step (d) as initial data, solve the equations (4.1) for $0 \leqslant \alpha \leqslant 1$. Once again, one step is sufficient.

(f) Now multiply the urea permeability of the vasa recta by 10 and repeat step (c).

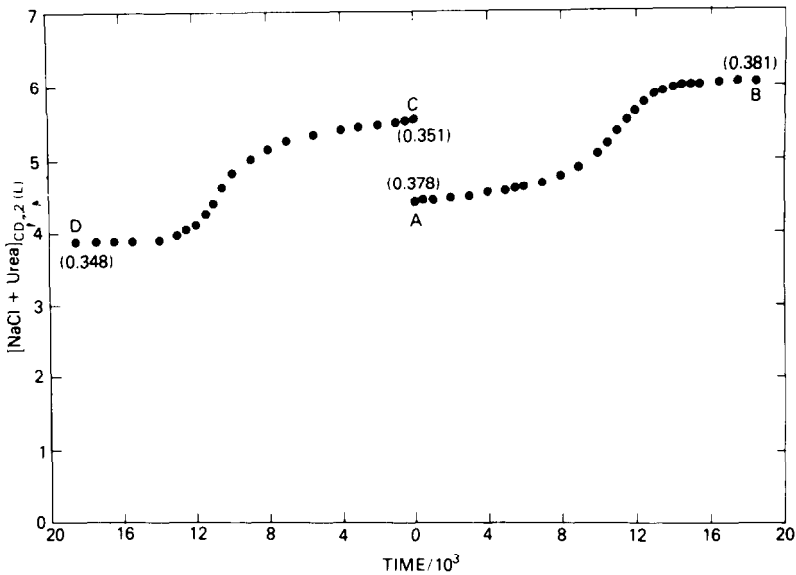(g) Repeat step (f) until the problem is solved.

FIG. 6. Time course of the transitions $A \rightarrow B$ and $C \rightarrow D$ shown in Figure 5. Numbers in parentheses indicate normalized values of the permeabilities. Note that the transitions $A \rightarrow B$ and $C \rightarrow D$ are induced by the minute change of 0.003 in the normalized value.

6. RESULTS

Having obtained a solution to the model with the desired parameters, one may investigate the model as a function of one or more of its parameters by solving the equations (4.2). Or one may solve a transient problem using Equations (3.7) and (3.8). The result shown in Figures 3 through 6 were obtained by a combination of these procedures. Fig ᴇ 3 shows the total urine concentration for this model wi ⅃ the boun⒟ ⅃ conditions shown in Table 2 as a function of the ratic of ⅃...ical to juxtamedullary nephrons. No solution is shown for a ratio less than 2.5 or greater than 9, because the urea concentration in some nephron-vascular segments is less than the discretization error. Note also that as the ratio increases to a value between 5 and 6 to 1, the concentration ratio attains a maximum. This is due to the fact that as the ratio increases, urea becomes available to drive the passive concentrating mechanism in the inner medulla. As the ratio increases further, the non-reabsorbed solute delivered to the collecting ducts acts as an osmotic diuretic, and the concentration ratio is reduced [29].

Note, also, that around a ratio of 3 to 1 there are multiple solutions to the model. A time stability analysis shows that the middle branch of solutions is

TABLE 1

Normalized Parameters[a]

Tube[b]	h_v	$10^4 R$	σ	σ_p	h_s	h_u	
G	1400	2	0	1	1	1	$R_A = 10.5 \times 10^{-4}$
PGC	300	28.5	0	1	4	4	$R_E = 0.1 \times 10^{-4}$
DVR1	100	28.5	0	1	1000	1000	$R_0 = 250 \times 10^{-4}$
DVR2	100	2000	0	1	1000	1000	$D_{0s} = 1 \times 10^{-3}$
CAVR	100	4.9	0	1	10000	10000	$D_{0u} = 1 \times 10^{-3}$
AVR1	100	24.5	0	1	1000	1000	
AVR2	100	2000	0	1	1000	1000	
BC	0	0	1	—	0	0	
PT	—	7	—	—	—	—	$B = 0.5$
DHL	50	10	1	—	0	0	
AHL1	0	10	1	—	.05, .85[c]	0	$a = 0.6, 0,$[c] $b = 0.1$
AHL2	0	10	1	—	.05	0	$a = 1.3,$ $b = 0.1$
DN1	0.2	6	1	—	0	0	$a = 0.3,$ $b = 1$
DN2	0.2	6	1	—	0	0	$a = 0.45,$ $b = 1$
CD	0.5[d]	6	1	—	0	0, 0.02[e]	

[a] h_v = hydraulic permeability, σ = Staverman reflection coefficient for filtered solutes, σ_p = reflection coefficient for large solute not filtered, h_s = salt permeability, h_u = urea permeability, R_A = flow resistance afferent to glomerulus, R_E = flow resistance efferent to glomerulus, R_0 = resistance to flow in the interstitium, D_{0s} = diffusion constant for salt in the interstitium, B = fraction of filtrate reabsorbed in the proximal tubule, a = maximum rate of transport, b = Michaelis constant.

[b] G = glomerulus, PGC = postglomerular capillary, DVR1 = descending vas rectum for first (juxtamedullary) nephrovascular unit, CAVR = cortical ascending nephrovascular unit, BC = Bowman's capsule, PT = proximal tubule, DHL = descending loop of Henle's limb, AHL = ascending loop of Henle's limb, DN = distal nephron, CD = collecting duct.

[c] The first value refers to the outer medulla where $0 \leqslant x \leqslant 0.5$; the second refers to the inner medulla where $0.6 \leqslant x \leqslant 1$. For $0.5 < x < 0.6$ the value varies linearly.

[d] The hydraulic permeability of the second (cortical) nephron population has been varied.

[e] The first value holds for $0 \leqslant x \leqslant 0.4$,; the second holds for $0.6 \leqslant x \leqslant 1$. For $0.4 < x < 0.6$ the value varies linearly.

unstable while the upper and lower branches are stable. In addition, the total energy requirements of the two stable branches are within 5% of each other: well within apparent metabolic limits for the kidney. Thus, none of these solutions is excluded by these criteria.

Figure 4 shows the solution surface for the model when viewed also as a function of the collecting duct hydraulic permeability for the cortical population. A cut through the fold in this surface is shown in Figure 5, for a ratio of

TABLE 2

Normalized Boundary Values

$[NaCl]_{arterial}$	1.0
$[Urea]_{arterial}$	0.05
$[Large\ proteins]_{arterial}$	0.0038
$P_{arterial}$	1.3×10^{-2}
P_{venous}	1.0×10^{-3}
$P_{bladder}$	1.44×10^{-3}

TABLE 3

Auxiliary Parameters

Number of nephron populations	2
Nephrons per population 1 (long)	1
Nephrons per population 2 (short)	3[a]

[a] The number of cortical nephrons has been varied.

3.5 to 1. Once again the middle branch of solutions is time unstable, while the upper and lower branches are stable.

Experimentally the unstable portion indicated by the dotted line $A \rightarrow C$ would be unobservable. Instead, a slight increase in collecting duct hydraulic permeability at the turning point A would cause a dynamic transition from the lower stable solution to the upper stable solution. This is indicated by the arrow AB. Similarly, at the turning point C, a slight decrease in hydraulic permeability would cause a transition back to the lower stable solution at D. Dynamically the system would follow the hysteresis loop $ABCDA$. The dynamic course of the system in the transitions AB and CD is shown in Figure 6.

7. SUMMARY

By utilizing a combination of Newton and continuation methods, it is possible to find solutions of the difference equations describing a multisolute, multinephron kidney model. It is also possible to follow these solutions as a function of one or more of the parameters describing tubular or vascular transport in the model. These same solution techniques should extend to models of even greater complexity. Without a path following method, con- struction of a connected part of the solution manifold would be very difficult.

The solutions of this multisolute, multinephron kidney model show the same type of behavior found in simpler models [6]. Namely, the solution manifold is folded into three sheets: an upper and a lower stable sheet and a middle unstable sheet. At the turning point where the lower stable sheet is

connected to the unstable sheet, an arbitrarily small change in the continuation parameter (e.g. increment in the collecting duct hydraulic permeability) can cause a transition from the lower to the upper stable sheet. A finite decrement will then return the system to the turning point that connects the upper stable sheet to the middle unstable sheet; an arbitrarily small decrement then returns the system to the lower stable state.

The occurrence of such multiple solutions and hysteresis type phenomena in both prototype [6] and more detailed kidney models provides additional support for the speculation that physiologically important correlates may be found in the mammalian kidney.

APPENDIX

Given an estimate for γ_G^n, the equations (3.7) can be solved iteratively in the direction of flow [16]. At each spatial tube position, the algebraic system is solved using code generated by the algebraic symbol manipulator MACSYMA [12, 17], thus avoiding all matrix inversions. Applying the Newton-Kantorovich and implicit function theorems [21, 34] we solve Equations (3.7) and (3.8), with (3.8) solved iteratively as follows:

$$\gamma_G^{n,l+1} = \gamma_G^{n,l} - H_l \Gamma_l^{-1} \phi_G(\gamma_G^{n,l}), \qquad l = 0, 1, \dots, \qquad (A.1)$$

where $\Gamma_l e_i = \phi_G(\gamma_G^{n,l} + \Delta\gamma\, e_i) - \phi_G(\gamma_G^{n,l})$, $i = 1, 2, \dots, r$; e_i is the unit vector with 1 in position i, and r is the number of global variables. For Newton's method $H_l = \Delta\gamma\, E$, where E is the identity matrix of order r, and $\Delta\gamma$ is a small increment. For a secant method

$$H_l = \left(\gamma_G^{n,l} - \gamma_G^{n,l-1}, \dots, \gamma_G^{n,l-h+1} - \gamma_G^{n,l-h}, \Delta\gamma\, e_1, \dots, \Delta\gamma\, e_{r-h} \right),$$
$$h = 1, 2, \dots, l \leqslant r. \quad (A.2)$$

With a rank one update [21], the secant method may be written so that with $\Gamma_l \equiv (q^{l-1} \; \cdots \; q^{l-r})$ we have

$$\Gamma_{l+1} = \Gamma_l P + (q^l - q^{l-r}) e_1^T \qquad (A.3)$$

and

$$\Gamma_{l+1}^{-1} = P^{-1}\Gamma_l^{-1} - \frac{1}{\alpha} P^{-1}\Gamma_l^{-1}(q^l - q^{l-r}) e_1^T P^{-1}\Gamma_l^{-1}, \qquad (A.4)$$

where $\alpha = 1 + e_1^T P^{-1}\Gamma_l^{-1}(q^l - q^{l-r}) \neq 0$ and P is a permutation matrix.

Solution of (3.8) is initiated by solving Equation (A.1) using Newton's method. Subsequently if $\|\phi_G(\gamma_G^{n,l-1})\| / \|\phi_G(\gamma_G^{n,l})\| \geqslant 10$, we use the previous matrices, setting $\Gamma_l^{-1} = \Gamma_{l-1}^{-1}$, $H_l = H_{l-1}$. If $4 \leqslant \|\phi_G(\Gamma_G^{n,l-1})\| / \|\phi_G(\gamma_G^{n,l})\| < 10$,

we use (A.4) and the secant method described in (A.2) to solve (A.1). The process is terminated when the maximum norm $\|\phi_G(\gamma_G^{n,l})\| \leqslant M$ for M a small constant, e.g. $M \sim (10^{-5})$.

REFERENCES

1 B. Bunow and J. Kernevez, Numerical exploration of bifurcating branches of solutions to reaction-diffusion equations from immobilized enzyme kinetics, in *Instabilities, Bifurcation and Fluctuations in Chemical Systems* (L. E. Reichl and W. C. Schieve, Eds.) Univ. of Texas Press, 1982.

2 P. S. Chandhoke and G. M. Saidel, Mathematical model of mass transport throughout the kidney: Effects of nephron heterogeneity and tubular-vascular organization, *Ann. Biomed. Engrg.* 9:263–301 (1981).

3 S.-N. Chow, J. Mallet-Paret, and J. A. Yorke, Finding zeroes of maps: Homotopy methods that are constructive with probability one, *Math. Comp.* 32:887–899 (1978).

4 M. G. Crandall and P. H. Rabinowitz, Bifurcation, perturbation of simple eigenvalues, and linearized stability, *Arch. Rational Mech. Anal.* 52:161–180 (1973).

5 D. Foster, J. A. Jacquez, and E. Daniels, Solute concentration in the kidney—II. Input-output studies on a central core model, *Math. Biosci.* 32:337–360 (1976).

6 J. B. Garner, R. B. Kellogg, and J. L. Stephenson, Mathematical analysis of a model for the renal concentrating mechanism, *Math. Biosci.* 65:125–150 (1983).

7 J. A. Jacquez, D. Foster, and E. Daniels, Solute concentration in the kidney—I. A model of the renal medulla and its limit cases, *Math. Biosci.* 32:307–335 (1976).

8 H. B. Keller, Numerical solution of bifurcation and nonlinear eigenvalue problems, in *Applications of Bifurcation Theory* (P. H. Rabinowitz, Ed.), Academic, New York, 1977.

9 M. Kubiček, Dependence of solution of nonlinear systems on a parameter, Algorithm 502, *ACM Trans. Math. Software* 2:98–107 (1976).

10 P. Lory, Numerical solution of a kidney model by multiple shooting, *Math. Biosci.* 50:117–128 (1980).

11 P. Lory, A. Gilg, and M. Horster, Renal countercurrent system: Role of collecting duct convergence and pelvic urea predicted from a mathematical model, *J. Math. Biol.* 16:281–304 (1983).

12 MACSYMA Reference Manual, The Mathlab Group, Laboratory for Computer Science, MIT, Dec. 1977.

13 R. Mejia, R. B. Kellogg, and J. L. Stephenson, Comparison of numerical methods for renal network flows, *J. Comput. Phys.* 23:53–62 (1977).

14 R. Mejia, J. L. Stephenson, and R. B. Kellogg, Comparison of numerical methods in solving renal countercurrent equations, in *Proceedings 1976 Summer Computer Simulation Conference*, pp. 502–506.

15 R. Mejia and J. L. Stephenson, Coned multinephron kidney model (Abstract), *Biophysical J.* 21:92a (1978).

16 R. Mejia and J. L. Stephenson, Numerical solution of multinephron kidney equations, *J. Comput. Phys.* 32:235–246 (1979).

17 R. Mejia and J. L. Stephenson, Symbolics and numerics of a multinephron kidney model, in *1979 MACSYMA User's Conference*, (V. E. Lewis, Ed.), Washington, 1979, pp. 596–603.

18 R. Mejia and J. L. Stephenson, Multiple solutions of convection-diffusion equations describing the renal concentrating mechanism, in *Numerical Methods for Engineering*, GAMNI2, DUNOD, Paris, 1980, pp. 1003–1013.

19 R. Mejia, J. L. Stephenson, and R. J. LeVeque, A test problem for kidney models, *Math. Biosci.* 50:129–131 (1980).

20 L. C. Moore and D. J. Marsh, How descending limb of Henle's loop permeability affects hypertonic urine formation, *Amer. J. Physiol.* 239:F57–F71 (1980).

21 J. M. Ortega and W. C. Rheinboldt, *Iterative Solution of Nonlinear Equations in Several Variables*, Academic, New York, 1970.

22 R. F. Pitts, *Physiology of the Kidney and Body Fluids*, 3rd ed., Year Book Med. Pub., Chicago, 1974.

23 J. L. Stephenson, Concentration in renal counterflow systems, *Biophys. J.* 6:539–551 (1966).

24 J. L. Stephenson, Concentrating engines and the kidney: I. Central core model of the renal medulla, *Biophys. J.* 13:512–545 (1973).

25 J. L. Stephenson, Concentrating engines and the kidney: II. Multisolute central core systems, *Biophys. J.* 13:546–567 (1973).

26 J. L. Stephenson, Free-energy balance in renal counterflow systems, *Math. Biosci.* 21:299–310 (1974).

27 J. L. Stephenson, R. P. Tewarson, and R. Mejia, Quantitative analysis of mass and energy balance in non-ideal models of the renal counterflow system, *Proc. Nat. Acad. Sci. U.S.A.* 71:1618–1622 (1974).

28 J. L. Stephenson, R. Mejia, and R. P. Tewarson, Model of solute and water movement in the kidney, *Proc. Nat. Acad. Sci. U.S.A.* 73:252–256 (1976).

29 J. L. Stephenson and R. Mejia, Effect of coning on the passive concentrating mechanism of the mammalian kidney (Abstract), *Fed. Proc.* 37:518 (1978).

30 J. L. Stephenson and R. Mejia, Salt, water and urea movement in a multinephron model of the mammalian kidney, in *Proceedings of the International Symposium on Mathematical Topics in Biology*, Research Institute for Mathematical Sciences, Kyoto Univ., Kyoto, Japan, 1978, pp. 78–87.

31 J. L. Stephenson, R. Mejia, and B. Kellogg, Multiple solutions in models of the renal medulla (Abstract), *Fed. Proc.* 39:1710 (1980).

32 J. L. Stephenson, Case studies in renal and epithelial physiology, in *Mathematical Aspects of Physiology* (Frank C. Hoppensteadt, Ed.), Lectures in Applied Mathematics, Vol. 19, Amer. Math. Soc., Providence, R.I., 1981, pp. 171–212.

33 R. P. Tewarson, A. Kydes, J. L. Stephenson, and R. Mejia, Use of sparse matrix techniques in numerical solution of differential equations for renal counterflow systems. *Comput. Biomed. Res.* 9:507–520 (1976).

34 R. P. Tewarson, J. L. Stephenson, and L. L. Juang, A note on solution of large sparse systems of nonlinear equations, *J. Math Anal. Appl.*, 63:439–445 (1978).